Sensors and Actuators A 172 (2011) 475–482

Contents lists available at SciVerse ScienceDirect

Sensors and Actuators A: Physical

journal homepage: www.elsevier.com/locate/sna

An efficient electromagnetic power harvesting device for low-frequency applications

Emilio Sardini, Mauro Serpelloni*

Department of Information Engineering, University of Brescia, Brescia, Italy

ARTICLE INFO

Article history:
Received 20 May 2011
Received in revised form 7 September 2011
Accepted 7 September 2011
Available online 28 September 2011

Keywords:
Low frequency vibrations
Energy harvesting
Non-linear generators
Electromagnetic generators
Power harvesting
Planar inductors
Human-powered devices
Energy scavenging
Micropower generator
Nonlinear oscillation

ABSTRACT

Mechanical energy in the form of low frequency vibrations (1–100 Hz) can be commonly available and this energy type can be advantageously converted to electrical one by exploiting energy harvesting techniques. At the same time, in many applications, the devices that convert low frequency mechanical energy to electrical one should have a small size. An electromechanical power generator is proposed for converting mechanical energy in the form of low-frequency vibrations, available in the measurement environment, into electrical energy. The intended applications for the proposed electromechanical power generator, described in this paper, are for examples mechanical systems with low frequency vibrations (1–100 Hz). The operating principle is based on the relative movement of a planar inductor with respect to permanent magnets. The generator implements a novel configuration of magnets that is proposed and analyzed with the aim to improve the conversion efficiency, increasing the spatial variation of magnetic flux. Furthermore, the generator uses polymeric material as resonators, which have low-frequency mechanical resonances due to the low Young's modulus of the materials by which they are made. The different materials, with which the suspensions for the planar inductor were made, have allowed to compare different behaviors of the resonators: linear and nonlinear. The experimental results have shown, for a linear resonator, a vibration frequency of about 100 Hz with generated powers of about 290 μW and a harvesting effectiveness of 0.5%, while, for the polymeric resonator made by Latex, the vibration frequency is around 40 Hz with a maximum power of 153 μW and a harvesting effectiveness of 3.3%. The proposed configuration can be adopted for its low profile, modularity and low-frequency vibrations in many applications from industrial to medical.

1. Introduction

Autonomous sensors are increasingly used in many applications for measurement of quantities either in mobile devices or in applications where the electrical energy is absent or the sensor cannot be connected by wires to the acquisition unit. Considering the characteristics of such systems, one major challenge is the energy source. For long-living systems, energy scavenging from ambient sources through power harvesting devices is an attractive alternative to batteries, which require periodical maintenances and also have disposal problems. Even if different types of energy are studied as energy input to the power harvester, the mechanical energy from vibrations is the most common energy source, the human and machine motions are particularly attractive energy sources and examples are reported in the literature [1,2]. The different technologies to convert mechanical energy in electrical energy include piezoelectric, electromagnetic systems and electrostatic systems. There are numerous issues that must be taken into consideration for a proper design of a power harvesting module that harvests energy form vibrations. One of the most significant issue concerns the frequency of mechanical vibrations: in a lot of application fields, from industrial to the medical, the frequencies are often low; examples are reported in the literature [3–6]. In [3], a linear energy harvester, which uses three permanent magnets, a resonant beam, and three coils, is described. It has a low-frequency resonance (369 Hz) and produces a power of about 0.6 μW for 14 μm exciting vibration amplitude and 0.4 mm gap between the magnets and coils. The volume is about 3.2 cm^3 and 0.6 g resonator mass. Paper [4] describes an electromagnetic generator, which was mounted on a man below the knee, to convert mechanical energy during walking. The system has a volume of about 0.5 cm^3, 1.37 g resonator mass and 1.8 mm as displacement, and the output power is intermittent with a mean output power of about 35 μW. In the literature, several authors propose a different approach based on the nonlinear behavior of the harvesting system; the aim is to decrease the volume and contemporarily increase the output power [5,6]. Paper [5] presents an electromagnetic generator that uses a frequency up-conversion technique: low-frequency

* Corresponding author. Tel.: +39 0303715543; fax: +39 030380014.
E-mail address: mauro.serpelloni@ing.unibs.it (M. Serpelloni).

0924-4247/$ – see front matter © 2011 Elsevier B.V. All rights reserved.
doi:10.1016/j.sna.2011.09.013

environmental vibrations are converted to a higher frequency through a mechanical frequency up-converter, and hence provides more efficient energy conversion. The system has a volume of about 6.4 cm^3, 120 nW output power and 64 Hz exciting vibration amplitude. In [6], an energy harvester allowing the use of nonlinear oscillations of magnetic levitation is proposed. The system uses the nonlinear restoring forces to lower the resonant frequency and tune the system resonance. The system has a 19.5 g resonator mass, 36.3 mm mass displacement and 12 Hz exciting vibration amplitude. The authors demonstrate that nonlinear phenomenon could be exploited to improve the effectiveness of energy harvesting devices. The investigation reveals that engaging the nonlinear response of system can result in relatively large oscillations over a wider range of frequencies, thus potentially improving the ability to harvest energy under certain circumstances.

Lowering the resonant frequency increases the geometric dimensions of the resonating element of the power harvester, making the systems too big for the required application. In fact, in the case of low-frequency vibrations, it is necessary to consider two conflicting demands; firstly the resonant frequency reduction requires an increase in mass and softness of the spring, against the size reduction requiring structural stiffening and an obvious reduction in mass.

In this paper, a proposal for lowering the mechanical frequency keeping low the geometric dimensions is reported. The decreasing in resonant frequency is obtained because the decrease in spring constant which is due to specific materials with low Young's modulus. The use of polymeric materials for the fabrication of the resonator has allowed the lowering of the damping constant, thus lowering the resonant frequency from about 100 Hz for a resonator made by FR4 to about 30 Hz for a polymeric resonator. Different polymeric materials were tested and different resonators were built. These materials can also have a nonlinear behavior [7]. The proposed harvester is an electromechanical power generator with a specific configuration of the magnets, which improves the conversion efficiency, increasing the spatial variation of magnetic flux. In a previous work [8], an electromagnetic generator employing a planar inductor has been described; the magnet configuration is preliminary analyzed and the experimental results show a linear behavior. The applications for the proposed electromechanical power generator described in this paper are for examples mechanical systems with low frequency vibrations (1–100 Hz), like air conditioning unit or industrial air compressor unit, which have resonant peaks between 40 and 50 Hz with accelerations of 0.9–1.7 m/s^2 [9].

This paper describes the design and analysis of the electromagnetic generator. A mathematical model has been developed for the analysis of mechanical and electrical behavior, the experimental system and experimental results are reported. The generators have been built and tested using a specially designed experimental setup. In the following paragraphs some considerations and experimental results are reported.

2. Device description

A schematic structure of the power harvesting device here proposed is shown in Fig. 1; it is constituted by two sets of magnets and a thin moveable structure between each set. The moveable structure, over which a flat inductor is fabricated, oscillates between the two sets. The magnets and the outer circular edge of the resonator are bounded rigidly to the case structure by circular supports that are not shown in Fig. 1 as they are used only for fixing. As shown in Fig. 1, the resonator is fixed by its external edge at the cylindrical case and it is placed symmetrically between the two sets of magnets. The case structure in Teflon has a cylindrical form with a diameter of 28 mm and a height of 14 mm and fixes rigidly the magnets.

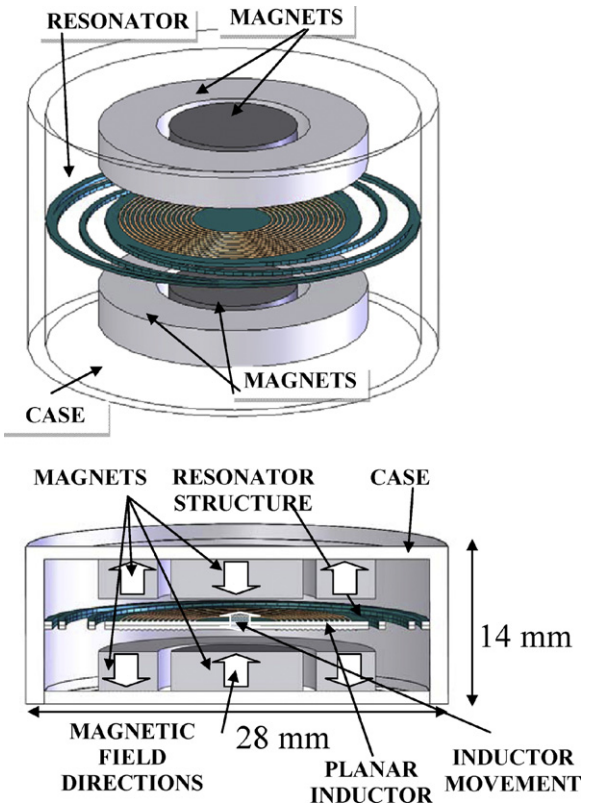

Fig. 1. Electromagnetic generator structure.

2.1. Resonators

Different materials and shapes were tested to investigate on the performance of the power harvesting generator. Two resonator structures, were designed (they are mentioned as A, B), and their photos with details about their shapes and dimensions are reported in Fig. 2(a) and (b). The shapes A and B are tied to the supporting structure by four beams and they resonate orthogonally to the shape plane due to geometrical symmetries. Shape B differs from A in the length of the supports; B has the shortest supports. Shape A has a lower mechanical resonant frequency than shape B. The resonators are made of different materials whose characteristics are reported in Table 1 (h is the thickness and E is the Young's modulus).

It was decided to introduce, for comparison purposes, a resonator with shape A obtained with the FR4 substrate to compare the resonance frequency maintaining the dimension and shape equal to the polymeric resonator. In the upper-left corner of Fig. 2(b) the resonator fabricated by printed circuit board (PCB) technology is reported. The PCB shape was easily fabricated exploiting microcutting techniques using FR4 substrate.

Table 1
Material properties.

Materials	h [mm]	E [MPa]
Vulkollan	1	14–30
Silicone	1	14–30
Latex	0.5	10–70
Para	0.5	10–100
PTFE	0.5	500
FR4	0.3	$1–25 \times 10^3$

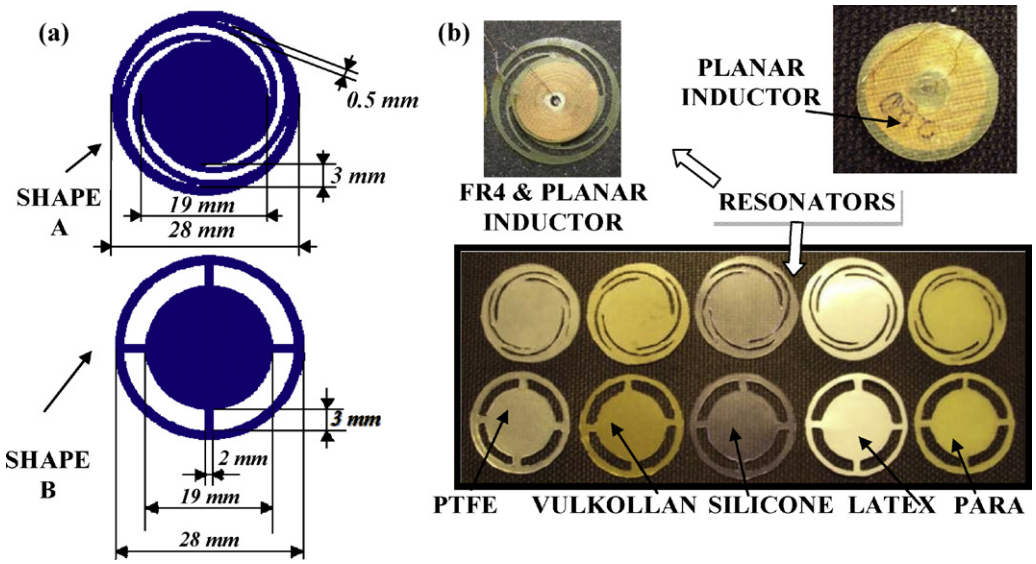

Fig. 2. Two resonator structures (a) and resonator components and planar inductors photos (b).

The polymeric resonators have two shapes A and B (Fig. 2(b), below). Four polymers were chosen: PTFE (Teflon), Vulkollan, Silicone, Latex, Para. The last four materials are elastomers, more commonly known as gums. These materials are isotropic, elastic and incompressible defined by hyperelastic law. Elastomers generally have a nonlinear elastic coefficient. In fact for them is not typically defined as a Young's modulus (E) that uniquely characterizes the material. The curve stress–strain varies continuously because the curve is not linear. The other material (PTFE) is a plastic.

For each fabricated resonator an identical planar inductor was glued to the resonator. The planar inductor is reported in the low-right corner and has been fabricated using a copper wound wire with a diameter of 0.1 μm (Fig. 2(b)). The planar inductor has 280 windings, an internal diameter of 5 mm and an external diameter of about 19 mm. The equivalent circuit parameters have been measured by an impedance analyzer (HP4194A). The fabricated inductor can be modeled with a series of an inductance and a resistance, both in parallel with a capacitance. The resistance is 22.51 Ω, the inductance is 242 μH and the capacitance is 9.5 pF.

2.2. The permanent magnet

The adopted Neodymium (NdFeB – N35) magnets are schematically shown in Fig. 1. The dimensions of the cylinder and ring magnets were chosen considering the dimensions of the resonators. The thickness of the magnets is 2.5 mm. The ring magnets have an inner diameter of 12 mm and an outer diameter of 20 mm, while the disc magnets have a diameter of 5 mm.

The magnetic field density distribution has been analyzed. The goal is to analyze different configurations of the magnetic field given by different arrangements of the magnets in order to identify the most efficient configuration for this application. Four different dispositions of the magnets, reported in Fig. 3, have been taken into consideration: they have been called Equal Vectors, Mixed Vectors, Opposite Vectors and Symmetric Vectors. In the Equal Vectors

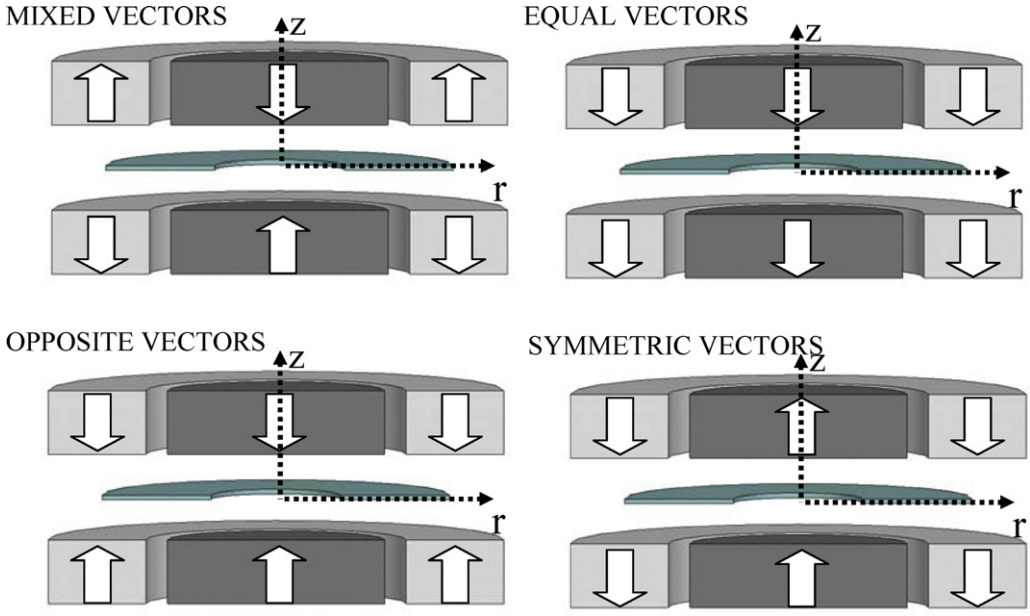

Fig. 3. Magnets configurations.

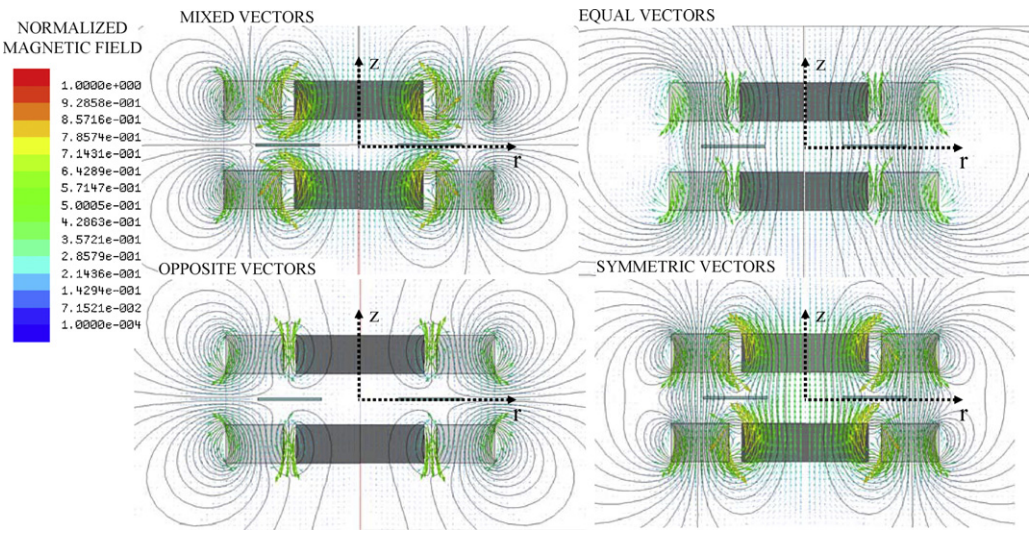

Fig. 4. Simulation plot in electromagnetic domain.

scheme, the upper and lower sets of magnets have the same direction of the magnetization vector. In the Opposite Vectors scheme, the upper magnets have the same direction of the magnetization vector, while the lower have an opposite direction. In the Symmetric Vectors scheme, the central magnets have the same direction of the magnetization vector, while the laterals have an opposite direction. In the Mixed Vectors scheme, the two central magnets have opposite magnetization vectors, while the two external magnets have opposite magnetization vectors, but also the external magnets have Opposite Vector with respect to the central one. Finite Element Methods (FEM) simulations of their configurations have been performed using Ansoft's Maxwell3D software. In Fig. 4, the B-field plots show the adopted Mixed Vectors solution compared with other spatial dispositions. With the aid of Maxwell3D, a FEM that uses a transient simulation has been implemented; the internal resonator was allowed to move up and down along the central axis between the magnets with a sinusoidal expression having a frequency of 100 Hz. The resonator is positioned exactly halfway between the magnets at the initial time t_0. An increase in efficiency requires that the distribution of magnetic field lines in the space between the magnets must be properly designed. The volume between the magnets is occupied by the movement of the resonator. This movement is assumed in first approximation a rigid translation of the resonator parallel to the magnets. The variation of the flow lines of the magnetic field that affects the area of the resonator must be highest to get a good-induced electromotive force (e.m.f.). To achieve this, the Mixed Vector configuration generates flow lines parallel to the magnets and the resonator with an improved spatial density than other configurations. The electromotive forces have been calculated for the four different configurations and the results are reported in Fig. 5; the Mixed Vectors configuration improves considerably the electromotive force (e.m.f.).

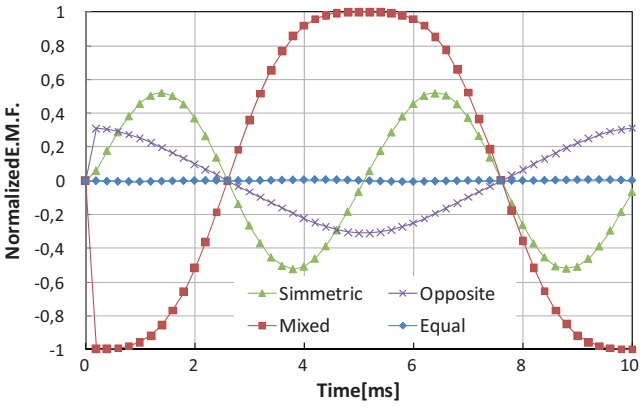

Fig. 5. Simulations results of electromotive force using different configurations of the magnets.

3. Modeling

Fig. 6 shows the diagram adopted for the modeling, where k is the spring elastic coefficient, c is the damping coefficient of damper, m is the oscillating mass, x is the same position with respect to an absolute reference, and y is the mechanical stress (related to the same reference x). A mechanic harmonic stimulus has been considered as base excitation, i.e. sinusoidal signals in the form $y = Y \sin \omega t$.

Depending on the type of material used and the amplitude of mechanical stimulus, the model can be linear or nonlinear. The FR4

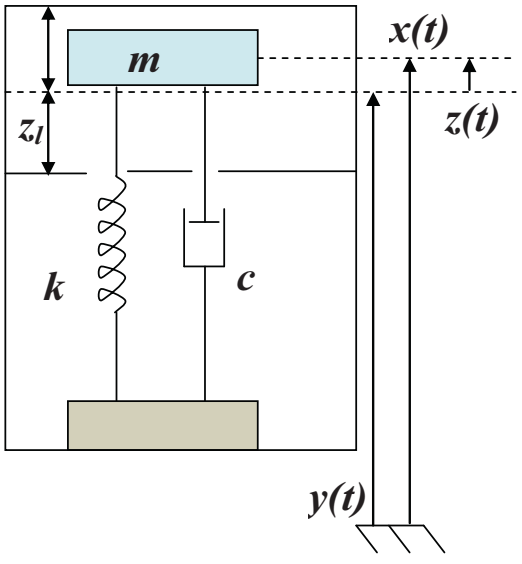

Fig. 6. Electromagnetic generator mechanical model.

resonator has a linear behavior due to the fact that the equivalent spring can be represented by an elasticity constant k for the amplitude.

For a harmonic excitation of the base $y = Y \sin \omega t$ and considering z the relative position of the resonator with respect to the base, the mechanical resonant frequency is given by [10]:

$$\omega_r = \frac{\omega_n}{\sqrt{1 - 2\xi^2}} \tag{1}$$

where $\omega_n = \sqrt{k/m}$ is the natural frequency, m is the mass and k the spring constant. Lowering the resonant frequency without increasing the device geometric dimensions and the damping ratio requires to decrease the spring constant k by choosing material that has lower value of the Young's modulus (E). In fact:

$$k = \frac{EWh^3}{4L^3} \tag{2}$$

where W, L and h are respectively width, length and thickness of the resonator.

Some materials used belong to a subset of elastic materials. Their elastic spring coefficient (k) has lower values than the FR4. This translates into lower resonance frequency since the natural frequency (where m is the mass of the element oscillating); the decrease of k implies a decrease in resonant frequency. Furthermore, the polymeric resonators have higher mass compared to the FR4 resonator. These materials present, however, a very important feature, their k is not constant. Then the resonator has been modeled as a spring-mass-damper system in which there is a damper, and a nonlinear spring, with a nonlinear coefficient (k_3). The g-force is considered 9.81 m/s^2. Eq. (3) reports the equation of the nonlinear spring:

$$F = kz + k_3 z^3 \tag{3}$$

Consequently, the mechanical equation takes the form,

$$m\ddot{z} + c\dot{z} + kz + k_3 z^3 = mg + m\omega^2 Y \ \sin \omega t \tag{4}$$

Dividing both sides by m, and taking a first change of variables,

$$\ddot{z} + \frac{c}{m}\dot{z} + \frac{k}{m}z + \frac{k_3}{m}z^3 = g + \omega^2 Y \ \sin \omega t \tag{5}$$

$$\ddot{z} + 2\xi\omega_n\dot{z} + \omega_n^2 z + \beta z^3 = g + \omega^2 Y \ \sin \omega t \tag{6}$$

Then, introducing the following substitutions: $2\xi\omega_n = 2\varepsilon\mu$, $\beta = \varepsilon\alpha$, $\omega^2 Y = 2\varepsilon\hat{Y}$, Eq. (6) assumes the following expression,

$$\ddot{z} + 2\varepsilon\mu\dot{z} + \omega_n^2 z + \varepsilon\alpha z^3 = g + 2\varepsilon\hat{Y} \ \sin \omega t \tag{7}$$

To find the frequency response of the system by the motion law a perturbation method of multiple scales [6] is applied. It is a mathematical method that allows to obtain an approximate solution of nonlinear problem, and, in order to obtain a more accurate analysis, it is restricted to frequencies close to the resonance of the system. The frequency of excitation signal is expressed as shown in Eq. (8), where σ is a parameter that indicates the closeness of the frequency of stimulation to the resonance (also called detuning parameter).

$$\omega = \omega_n + \varepsilon\sigma \tag{8}$$

The mathematical method used, clearly reported in [6], leads to get the first approximation of the solution, thus:

$$z = a \ \sin(\Omega t - \gamma) \tag{9}$$

where γ is a constant that is imposed to arrive at the steady-state solution.

The relationship of "a" (the amplitude of oscillation on the base of the vibrating element) to σ (the frequency deviation from the natural frequency of the system) can be obtained using the method reported in [6], thus:

$$\left[\mu^2 + \left(\sigma - \frac{3\alpha}{8\omega_n}\left(a^2 + 4\frac{g^2}{\omega_n^4}\right)\right)^2\right] a^2 = \frac{\hat{Y}^2}{\omega_n^2} \tag{10}$$

From Eq. (10), it is possible to obtain the frequency response of the system. To draw such a curve, Eq. (10) is solved for σ in terms of "a". The approach gives,

$$\sigma = \frac{3a\alpha(a^2\omega_n^4 + 4g^2) \pm 8\omega_n{}^4\sqrt{\hat{Y}^2 - (a\mu\omega_n)^2}}{8a\omega_n^5} \tag{11}$$

Eq. (11) permits to study the relationship of the peak amplitude with the model quantities, which, in the first approximation, solving Eq. (11) and substituting the previous expression, depends proportionally by Y (amplitude of the mechanical stimulus), Ω (frequency of the mechanical stimulus) and m (mass). Furthermore, Eq. (11) can be rewritten using Eq. (8) and expressions used before. Then, the expression that relates the frequency (ω) with the amplitude (a) can be obtained.

$$\omega = \frac{8a\omega_n^6 + 3a\beta(a^2\omega_n^4 + 4g^2) \pm 8\omega_n^4\sqrt{\left(\omega^2 Y/2\right)^2 - \left(a\xi\omega_n^2\right)^2}}{8a\omega_n^5} \tag{12}$$

The mathematical model was simulated using Matlab. In Fig. 7, the simulation results of the mathematical model is reported; using the data reported in figure and imposing a value of "a", the model gives the values of ω.

Repeating the calculation for a range of values of a, and combining the real solutions, the evolution in amplitude of oscillation frequency of the resonator was obtained (blue-continuous line). The simulation results are interpreted with a jump; for a real system the increasing frequencies (green line) and a decrease (red line) generate a jump in the function.

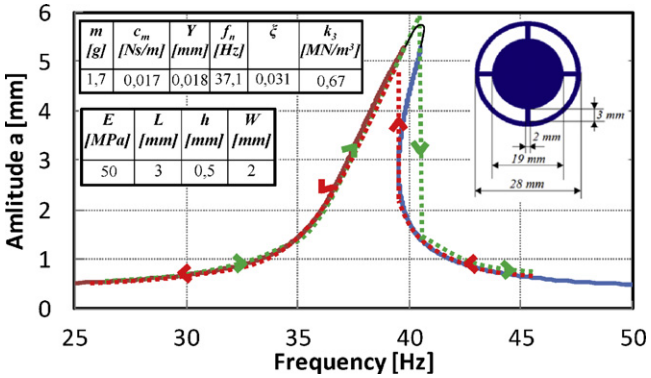

Fig. 7. Simulation results of the mathematical model implemented. The two sets of data obtained from Eq. (11) are reported in blue and red. The red and green dot lines represent the decreasing and increasing frequency path, respectively. (For interpretation of the references to color in this figure legend, the reader is referred to the web version of this article.)

4. Experimental system

In Fig. 8, the block diagram of the experimental setup for testing of the fabricated prototypes is reported. In Fig. 8, the generator is reported centrally, the generator is the device that contains the vibrating membrane (resonator). An electrodynamic shaker (Bruel & Kjaer 4290) is used to produce mechanical vibrations to the generator under test. The sinusoidal excitation is supplied by a function generator (Agilent 33220A) programmed by PC using the GPIB bus. Each resonator was tested inside the generator case using the fabricated planar inductor and fixed on the shaker using a designed

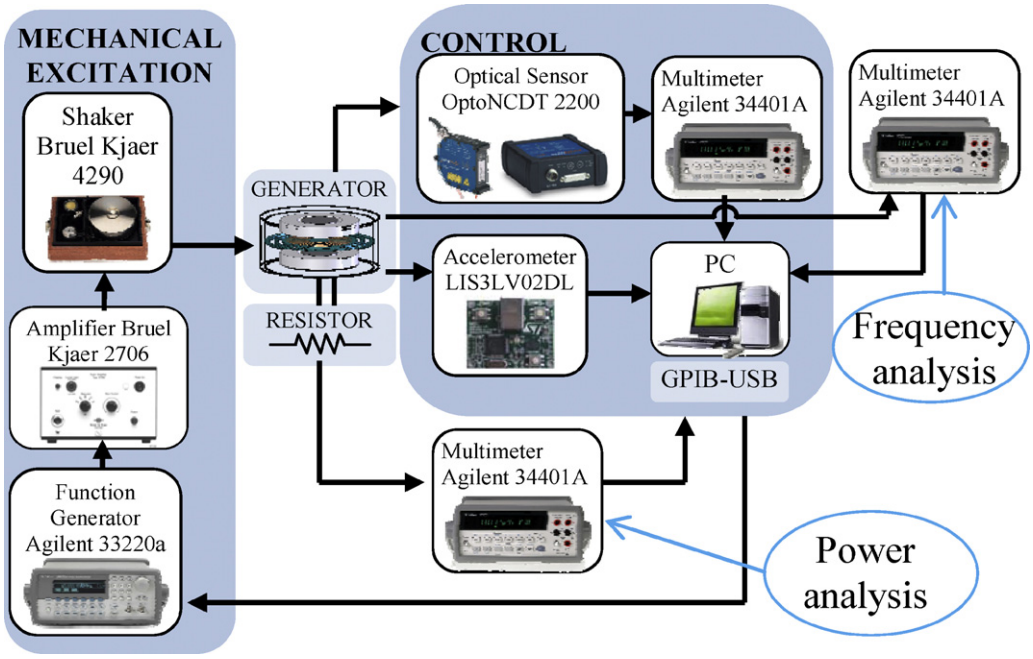

Fig. 8. Block diagram of the experimental setup for the controlled vibration system.

screw clamp. Two different analyses have been undertaken, a frequency analysis to study the mechanical resonant frequency of the resonator and a power analysis to study the behavior with different resistive loads of the generator. The vibration amplitude, as a function of frequency of each prototype, has been recorded by an optical sensor (OptoNCDT 2200), whose output was measured by a multimeter (Agilent 34401A) connected to the PC with a GPIB cable. A power analysis has been conducted as well; a 3-axis accelerometer (LIS3LV02DL) and the conditioning electronics (STEVAL-MKI005V1) were mounted axially above to provide a control on the vibration amplitude of the generator. The generators output was applied across a resistive matched load and the voltages were measured by a multimeter (Agilent 34401A). All the instruments are connected by GPIB to the PC where LabVIEW software coordinates the measurement activities.

5. Experimental results

The experimental tests permitted to analyze the performance of the generators designed with the different proposed resonators. All the experimental results were carried out setting the maximum acceleration of the system at about 9.81 m/s^2.

In the first step, the linear resonator (shape A) were mounted, one at a time, in the generator case and tested; the generator output voltage for different frequencies and with a resistive load of 1 MΩ is reported in Fig. 9(a). Furthermore, the diagram in Fig. 9(a) has been compared with the resonant frequency analysis obtained with the optical system, showing a good agreement. The considerations given in Section 3 permit to observe that a method to discern between a non-linear resonant system and linear one is analyzing the deviation to the right or left of its resonance curve. The more

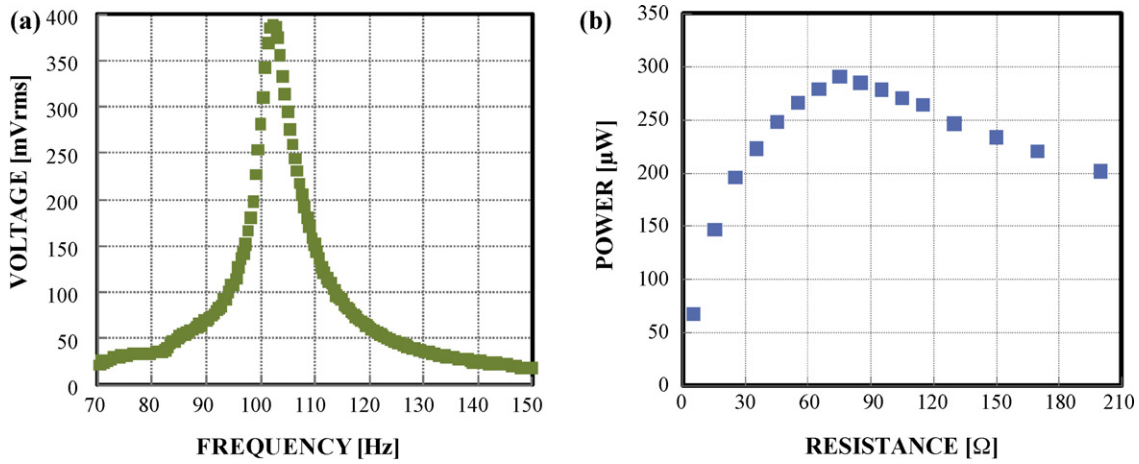

Fig. 9. Output voltages for the generator for different frequencies at 1-MΩ load resistance (a) and output power of the generator for different load resistances at mechanical resonance (b).

Table 2
Experimental results for the linear generators.

Generator	Mechanical resonance [Hz]	Quality factor Q	Load resistance [Ω]	Power at resonance [μW]	Voltage at resonance [mV]
FR4	102	20.4	76	290	183.2

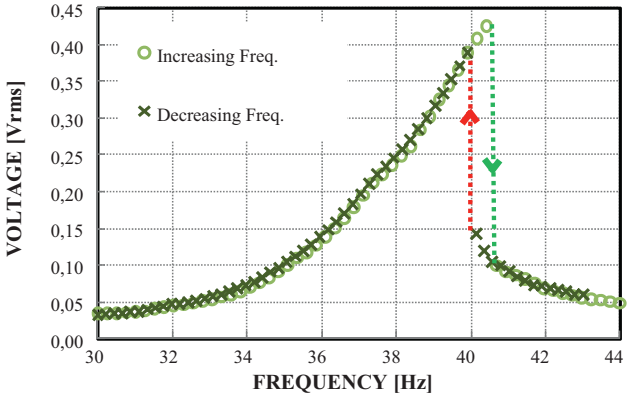

Fig. 10. Experimental data obtained increasing and decreasing the stimulus frequency (Latex), the two jumps are reported as dot lines.

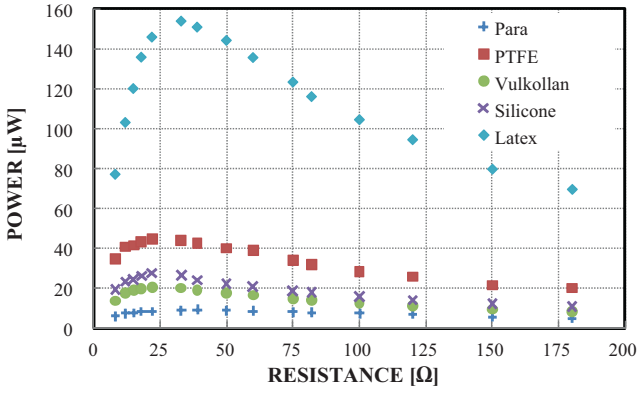

Fig. 12. Output power of the generators for different load resistances at mechanical resonances.

the system is not linear, the more the curve will be diverted to the right or left. Referring at Fig. 9(a), it can be deduced that curve have the typical behavior of a linear resonant system.

Whereas, the resonator can operate at their mechanical resonant frequency with an acceleration of 9.81 m/s^2, different resistive loads were connected to the generators for analyzing the power flowing into the load. In Fig. 9(b), the output power of the generator, measured at its resonant frequency, versus different load resistances is reported. The diagram has a maximum output power of about 290 μW, which can be observed for a load of 76 Ω.

In Table 2, a comparison of the measured characteristics of the generator is given. The frequency characterization has permitted evaluating the resonant frequencies and the quality factor for the resonator, while the voltage and power at resonance of the generators have been extracted from Fig. 9(b). The quality factor for the devices was calculated considering that the ratio of the resonant frequency and the difference between the 3-dB frequencies at each side of the resonance.

Several tests were performed on resonators made of polymer material as well. In Figs. 11 and 12, and in Table 3 reported below, the experimental data of generators are labeled as the polymeric material of the resonators that makes them. The most significant data are reported and concern Para and Latex, having shape B, while the others have shape A. Using the experimental system designed,

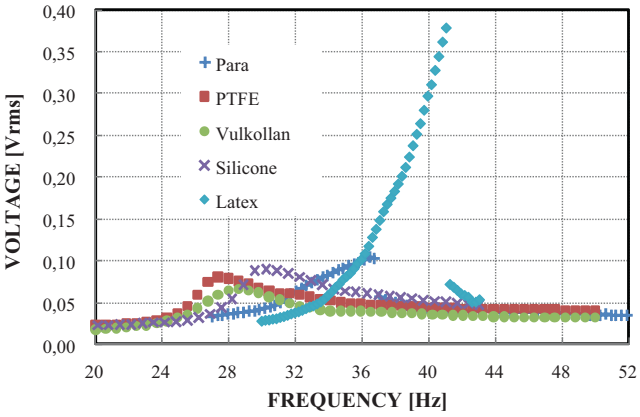

Fig. 11. Output voltages of the generators for different frequencies.

a frequency analysis was done to analyze the behavior of the polymeric resonators. In Fig. 10, the experimental results obtained with Latex are reported. The diagrams are obtained increasing and decreasing the stimulus frequency.

In Fig. 11, the trends for all the generators mounting polymeric resonators are shown. The resonators made with Latex and Para have a strongly nonlinear behavior permitting high amplitudes; due to nonlinear behaviors, Para and Latex show the highest output voltages. The use of polymeric materials for the resonator realization has allowed the lowering of the resonant frequency. All the resonators have lower resonant frequencies than in linear case. In Fig. 12, diagrams of the generated power with different applied loads are shown. Latex generates about 0.16 mW at 30 Hz, the data are reported in Table 3 as well. The strong nonlinearity of the Latex resonator permits much higher output power than the other.

Considering the generator from Table 1 (FR4) and the best from Table 3 (Latex), a performance metric analysis was done. Using the performance metrics described in [2], it is possible to obtain different parameters such as the Power Density equal to the ratio between the power and the volume or the Harvester Effectiveness (*HE*) which is mainly a measure of how closely a specific design approaches its ideal performances and it is defined as the ratio between the useful power output and the maximum possible output [2], thus,

$$\mathrm{HE} = \frac{P}{(1/2)Y_0 Z_l \omega^3 m} \tag{13}$$

where P is the measured power, m is the mass, Z_l is the half-distance between the two pairs of magnets, Y_0 is the input amplitude, and ω is the input frequency.

In Table 4, the power density of the linear is about 33.7 μW/cm^3 and the harvesting effectiveness is 0.5%. While the power density for the nonlinear generator is about 17.8 μW/cm^3 and the harvesting effectiveness is 3.3%. Compared to the power harvesting systems reported in [2], the proposed electromagnetic generator has a good match between low-resonant frequency and harvesting effectiveness. Furthermore, the lower resonant frequencies, due to polymeric resonator materials, give the possibility to harvest energy from low frequency vibrations, at about 40 Hz. The proposed nonlinear generator is a viable solution for applications that have resonant peak at about 40–50 Hz, like air conditioning unit or industrial air compressor unit.

Table 3
Generator results with frequency analysis.

Generators	Mechanical resonance [Hz]	Quality factor Q	Load Resistance [Ω]	Power at resonance [μW]	Voltage at resonance [mV rms]
Para	36.8	5.8	39	11.0	104
Silicone	27.3	1.3	22	27.0	81
Vulkollan	28.6	1.6	22	20.0	66
PTFE	30.2	1.8	22	44.0	90
Latex	41.0	12.4	33	153	378

Table 4
Generator comparison.

Generator	Generator volume [cm^3]	Proof mass [g]	Z_l [μm]	Input amplit. [μm]	Input freq. [Hz]	Power P [μW]	Power density [$\mu W/cm^3$]	Harvester Effectiveness HE%
Latex (Table 3)	8.6	2.1	3000	85	41	153	17.8	3.3
FR4 (Table 2)	8.6	1.5	3000	85	102	290	33.7	0.5

6. Conclusions

A nonlinear electromagnetic generator employing planar resonators for autonomous sensor applications has been presented. To improve the conversion efficiency from mechanical to electrical energy, different configurations of magnets were analyzed. The proposed mixed configuration guarantees the most efficient distribution of the flux lines as it increases the spatial variation of magnetic flux and was adopted for all the electromagnetic generators. A mathematical model was developed for the analysis of mechanical behavior, identifying the expression that relates the frequency of the excitation with the amplitude of the movement of the resonator. An experimental system was developed and several tests were performed. The fabricated resonators were analyzed and as expected the polymeric resonator showed lower-frequency mechanical resonances compared to the linear one due to the low Young's modulus of the materials. All the generators made by polymeric resonator showed a lowering of the resonant frequencies from about 100 Hz to about 30–40 Hz. Measurements on this system show that it is possible to generate maximum instantaneous power and voltage of 290 μW and 183 mV for the linear resonator at 102 Hz, while with the nonlinear resonator (Latex) it is possible to generate maximum instantaneous power and voltage of 153 μW and 378 mV respectively at 41 Hz. The proposed generators represent an interesting solution for powering low-power systems by using low-frequency vibrations.

References

[1] C.O. Mathuna, T. O'Donnell, R.V. Martinez-Catala, J. Rohan, B. O'Flynn, Energy scavenging for long-term deployable wireless sensor networks, Talanta 75 (2008) 613–623.
[2] P.D. Mitcheson, E.M. Yeatman, G.K. Rao, A.S. Holmes, T.C. Green, Energy harvesting from human and machine motion for wireless electronic devices, Proc. IEEE 96 (9) (2008) 1457–1486.
[3] B. Yang, C. Lee, W. Xiang, J. Xie, J.H. He, R.K. Kotlanka, S.P. Low, H. Feng, Electromagnetic energy harvesting from vibrations of multiple frequencies, J. Micromech. Microeng. 19 (2009) 8, 035001.
[4] T. Von Buren, G. Troster, Design and optimization of a linear vibration-driven electromagnetic micro-power generator, Sens. Actuators A 135 (2007) 765–775.
[5] H. Kulah, K. Najafi, Energy scavenging from low-frequency vibrations by using frequency up-conversion for wireless sensor applications, IEEE Sens. J. 8 (2008) 261–268.
[6] B.P. Mann, N.D. Sims, Energy harvesting from the nonlinear oscillations of magnetic levitation, J. Sound Vib. 319 (2009) 515–530.
[7] R. Ramlan, M.J. Brennan, B.R. Mace, I. Kovacic, Potential benefits of a non-linear stiffness in an energy harvesting device, Nonlinear Dyn. 59 (2010) 545–558.
[8] D. Marioli, E. Sardini, M. Serpelloni, Electromagnetic generator employing planar inductors for autonomous sensors applications, in: Proceedings of the Eurosensors XXIII conf. Lausanne, Proc. Chem. 1 (2009) 469–472.
[9] S. Roundy, P.K. Wright, J. Rabaey, A study of low level vibrations as a power source for wireless sensor nodes, Comput. Commun. 26 (2003) 1131–1144.
[10] N.G. Stephen, On energy harvesting from ambient vibration, J. Sound Vib. 293 (2006) 409–425.

Biographies

Emilio Sardini was born in Commessaggio, Mantova, Italy in 1958. He graduated in Electronic Engineering at the Politecnico of Milan, Italy, in 1983. Since 1984 he joined the Department of Information Engineering of the University of Brescia, Italy. Since 2006 he is a Full Professor in Electrical and Electronics Measurements. His research activity is in the field of sensors and electronic instrumentation; in particular he developed the conditioning electronics mainly for capacitive and inductive sensors, microprocessor based instrumentation, thick film sensors, instrumentation for noise measurement and for low frequency acceleration measurements. Recently the research interest has been addressed to autonomous sensor for biomedical applications. He is also a coordinator of the Technology for Health PhD.

Mauro Serpelloni was born in Brescia, Italy, in 1979. He received the Laurea degree (summa cum laude) in industrial management engineering and the Research Doctorate degree in electronic instrumentation from the University of Brescia, Brescia, in 2003 and 2007, respectively. He is currently a Research Assistant of electrical and electronic measurements with the Department of Information Engineering, University of Brescia. He has worked on several projects relating to the design, modeling, and fabrication of measurement systems for industrial applications. His research interests include biomechatronic systems, contactless transmissions between sensors and electronics, contactless activation for resonant sensors, and signal processing for microelectromechanical systems.